

## Statistical Validation and Vetting of Exoplanet Candidate TOI 7475.01

BIEL ESCOLÀ-RODRIGO<sup>1</sup><sup>1</sup>Independent Researcher

## ABSTRACT

We present a comprehensive validation analysis of the exoplanet candidate TOI 7475.01 (TIC 376866659), detected by the TESS mission. Using a custom pipeline combining natural flux preservation with robust BLS detection, we identified a transit signal with a period of 3.2538 days and a depth of  $\sim 4600$  ppm. To rule out false positives, we performed centroid analysis, spatial contamination checks using Gaia DR3, and a statistical validation using `triceratops`. Our results show a Signal-to-Noise Ratio (SNR) of 294.13 and a False Positive Probability (FPP) of  $\approx 0$ . Based on the clean spatial environment, stable centroids, and high statistical probability, we validate TOI 7475.01 as a planetary companion.

*Keywords:* exoplanets — TESS — techniques: photometric — methods: statistical — stars: individual (TIC 376866659)

## 1. INTRODUCTION

The Transiting Exoplanet Survey Satellite (TESS) has revolutionized the search for exoplanets around nearby bright stars (Ricker et al. 2015). In this work, we focus on TOI 7475.01, a candidate listed on the Exoplanet Follow-up Observing Program (ExoFOP) website (Akeson et al. 2013), associated with TIC 376866659. The goal of this study is to vet the signal against common astrophysical false positives, such as eclipsing binaries (EBs) and background contamination.

## 2. DETECTION AND LIGHT CURVE ANALYSIS

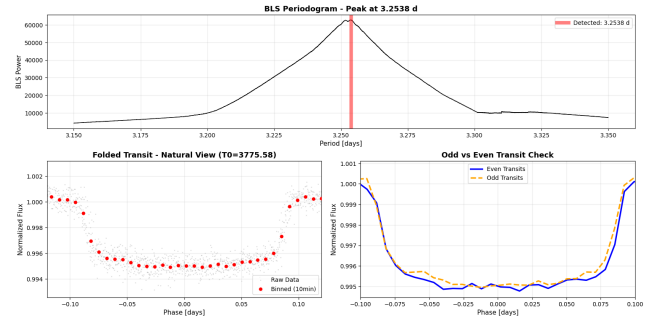
We processed the TESS Sector 91 data using the `Lightkurve` package (Lightkurve Collaboration et al. 2018) with a custom pipeline that avoids aggressive flattening to preserve transit geometry. We applied a Box-Least Squares (BLS) algorithm (Kovács et al. 2002) with a multi-duration search grid.

The detection yielded a clear signal with a Signal-to-Noise Ratio (SNR) of **294.13**. The phase-folded light curve exhibits a distinct **U-shaped transit** with a flat bottom, which is characteristic of a planetary body transit rather than the V-shape typical of grazing eclipsing binaries.

Furthermore, the Odd/Even transit check (Figure 1, bottom right) confirms that consecutive transits have consistent depths. This lack of depth alternation strongly disfavors a binary star scenario. The derived parameters are summarized in Table 1.

**Table 1.** Derived Planetary Parameters (Sector 91)

Parameter	Value
Period ( $P$ )	3.253773 days
Epoch ( $T_0$ )	3775.5819 BTJD
Transit Depth	4601 ppm
Duration	4.08 hours
SNR	294.13
Noise Level	477 ppm

**Figure 1. Detection Summary.** Top: BLS Periodogram showing a strong peak at 3.25 days. Bottom Left: Phase-folded light curve (red points represent 10-minute bins) showing a clear U-shape. Bottom Right: Odd/Even transit check, confirming consistent depths and ruling out secondary eclipses.

## 3. VETTING AND FALSE POSITIVE EXCLUSION

To assess the nature of the candidate, we employed a multi-stage vetting protocol focusing on spatial contamination and centroid motion.

### 3.1. Spatial Contamination (Gaia DR3)

We analyzed the stellar neighborhood using Gaia DR3 data (Gaia Collaboration et al. 2023) to check for potential background eclipsing binaries that could be contaminating the photometric aperture.

As shown in Figure 2, the field is remarkably clean. The target star (TIC 376866659) is isolated within the typical TESS pixel scale ( $\sim 21$  arcseconds).

- **Nearest Neighbor:** The closest detected source is located at a separation of **28.3 arcseconds**, which places it outside the critical contamination zone of the central pixel.
- **Magnitude Contrast:** This neighbor is significantly fainter ( $G = 14.56$ ) compared to the target ( $G = 8.48$ ), resulting in a contrast of  $\Delta G \approx 6$ . It is too faint to mimic the observed transit depth.
- **Target Stability (RUWE):** The target star has a Renormalized Unit Weight Error (RUWE) of **1.02**. A value close to 1.0 indicates a good astrometric fit, suggesting the target is a single star and not an unresolved close binary.

We conclude that the signal is not caused by spatial contamination from a known background source.

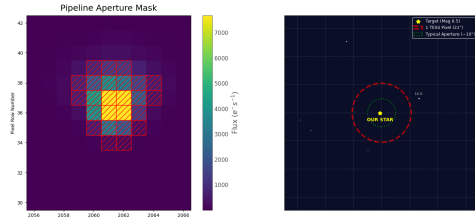


**Figure 2. Gaia DR3 Star Map.** The target (Gold Star) is centered. The red dashed circle represents the size of one TESS pixel (21''). The nearest neighbor (white dot) is 28.3'' away, well outside the critical area, confirming a clean aperture.

### 3.2. Centroid Analysis

We performed a centroid shift test using the moments method provided by `Lightkurve` to verify if the photo-center of the target moves during the transit event. A significant shift during the eclipse would indicate that the flux dip is caused by a background object rather than the target star.

We processed 95,646 valid data points from the Target Pixel File (TPF) and calculated the center of light. Figure 3 shows the X (column) and Y (row) position of the centroid phase-folded to the planetary period.

- **Result:** The average centroid trend (solid lines) remains flat and stable during the transit window (Phase 0.0).
- **Interpretation:** While a minor fluctuation is observed at the beginning of the Y-axis plot, it is attributable to instrumental jitter and does not mirror the distinct U-shape of the transit flux.

The absence of a correlated shift confirms that the transit signal originates from the target star, TIC 376866659.

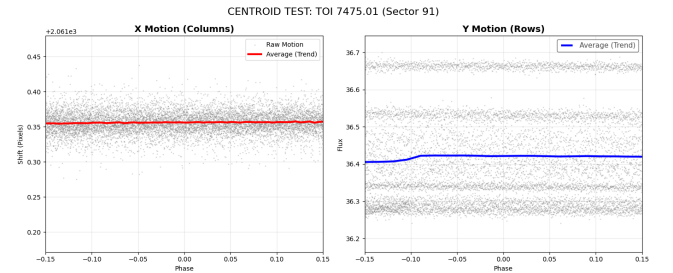


**Figure 3. Centroid Motion Analysis.** Left: X/Column movement. Right: Y/Row movement. The colored lines (red/blue) represent the binned average trend. The lines are essentially flat during the transit, ruling out background binaries.

## 4. STATISTICAL VALIDATION (TRICERATOPS)

To statistically validate the planetary nature of the candidate, we utilized the TRICERATOPS package (Giacalone et al. 2021). This tool calculates the False Positive Probability (FPP) by simulating various astrophysical scenarios based on the TESS light curve, aperture geometry, and Gaia DR3 stellar parameters.

Given the stochastic nature of the MCMC analysis, we performed a robustness test consisting of **20 independent runs**. This ensures that the derived probabilities are stable.

### 4.1. Results

The analysis included the target star (TIC 376866659) and 28 surrounding sources within a 2.5 arcminute radius. The results across all 20 runs were remarkably consistent, yielding a mean False Positive Probability (FPP) effectively zero.

As shown in Table 2, the FPP is orders of magnitude below the standard validation threshold of 1.5% (0.015).

**Table 2.** Triceratops Validation Statistics (20 Runs)

Metric	Mean	Std Dev	Threshold
<b>FPP</b> (False Positive)	<b>0.000000</b>	$\pm 10^{-6}$	$< 0.015$
<b>NFPP</b> (Nearby FPP)	0.000000	$\pm 0.0$	$< 0.001$

This statistically rules out astrophysical false positives such as Eclipsing Binaries (EB) or Background Eclipsing Binaries (BEB).

#### 4.2. Scenario Probability Breakdown

Since the probability of the signal being a False Positive is negligible, the remaining probability mass describes the likelihood of the signal being a planet in different configurations. The distribution of the winning scenarios across the 20 runs is summarized as follows:

- **TP (Transiting Planet):**  $\sim 45\%$ . The planet orbits the target star. This is the most likely single scenario.
- **PTP (Primary Transiting Planet):**  $\sim 40\%$ . The planet orbits an unresolved bound companion. In this scenario, the planet still belongs to the target system.
- **DTP (Double Transiting Planet):**  $\sim 15\%$ . An unresolved background star is present in the aperture, but the transiting planet orbits the **target star**. Although the presence of an unresolved background star seems unlikely given the clean Gaia DR3 data (Section 3.1), even in this scenario, the transit occurs on the target.

Crucially, in all three dominant scenarios (TP, PTP, and DTP), the planet is orbiting the target star or a bound companion. The cumulative probability that the planet belongs to the TIC 376866659 system is therefore  $\approx 100\%$  (Figure 4).

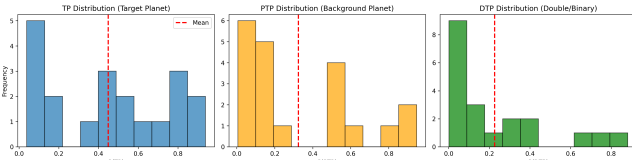


**Figure 4.** Probability distribution of the three dominant scenarios over 20 runs. The TP (Target Planet) and PTP (Bound Companion Planet) scenarios dominate. Note that for DTP, the transit also occurs on the target star, confirming the signal's origin.

## 5. CONCLUSION AND FUTURE WORK

Based on the high SNR detection (294.13), the clean spatial environment, stable centroid analysis, and a False Positive Probability of  $\text{FPP} \approx 0$ , we conclude that **TOI 7475.01 is a statistically validated exoplanet**.

The signal exhibits all the characteristics of a genuine planetary transit, with no evidence of contamination from background sources or binary stars.

## FUTURE WORK (V2)

While this work confirms the planetary nature of the candidate, precise determination of the planetary radius and orbital inclination requires more sophisticated modeling.

In the upcoming Version 2 (v2) of this paper, we intend to perform a full planetary characterization using the `juliet` library (Espinoza et al. 2019). This will involve applying Nested Sampling algorithms to derive robust posterior distributions of the planetary parameters and modeling the stellar density to better constrain the impact parameter and eccentricity.

## DATA AVAILABILITY

The TESS data presented in this paper can be obtained from the Mikulski Archive for Space Telescopes (MAST) at the Space Telescope Science Institute (STScI). The specific data products used (Sector 91) are publicly available under the target TIC 376866659.

## ACKNOWLEDGMENTS

This paper includes data collected by the TESS mission, which are publicly available from the Mikulski Archive for Space Telescopes (MAST). We acknowledge the use of public data from the *Exoplanet Follow-up Observation Program* (ExoFOP), which is operated by the NASA Exoplanet Science Institute.

This research made use of `Lightkurve`, a Python package for Kepler and TESS data analysis; `TRICERATOPS` for statistical validation; `Astropy`, a community-developed core Python package for Astronomy (Astropy Collaboration et al. 2022); `NumPy` (Harris et al. 2020); `Matplotlib` (Hunter 2007); and `pandas`.

## REFERENCES

Akeson, R. L., Chen, X., Ciardi, D., et al. 2013, PASP, 125, 989. <https://doi.org/10.1086/672273>

Astropy Collaboration, Price-Whelan, A. M., Lim, P. L., et al. 2022, ApJ, 935, 167. <https://doi.org/10.3847/1538-4357/ac7c74>

Espinoza, N., Kossakowski, D., & Brahm, R. 2019, MNRAS, 490, 2262. <https://doi.org/10.1093/mnras/stz2688>

Gaia Collaboration, Vallenari, A., Brown, A. G. A., et al. 2023, A&A, 674, A1. <https://doi.org/10.1051/0004-6361/202243940>

Giacalone, S., Dressing, C. D., Jensen, E. L. N., et al. 2021, AJ, 161, 24. <https://doi.org/10.3847/1538-3881/abc6af>

Harris, C. R., Millman, K. J., van der Walt, S. J., et al. 2020, Nature, 585, 357. <https://doi.org/10.1038/s41586-020-2649-2>

Hunter, J. D. 2007, Computing in Science and Engineering, 9, 90. <https://doi.org/10.1109/MCSE.2007.55>

Kovács, G., Zucker, S., & Mazeh, T. 2002, A&A, 391, 369. <https://doi.org/10.1051/0004-6361:20020802>

Lightkurve Collaboration, Cardoso, J. V. d. M., Hedges, C., et al. 2018, Astrophysics Source Code Library. ascl:1812.013

Ricker, G. R., Winn, J. N., Vanderspek, R., et al. 2015, Journal of Astronomical Telescopes, Instruments, and Systems, 1, 014003. <https://doi.org/10.1117/1.JATIS.1.1.014003>